Pankiv et al., http://www.jcb.org/cgi/content/full/jcb.200907015/DC1

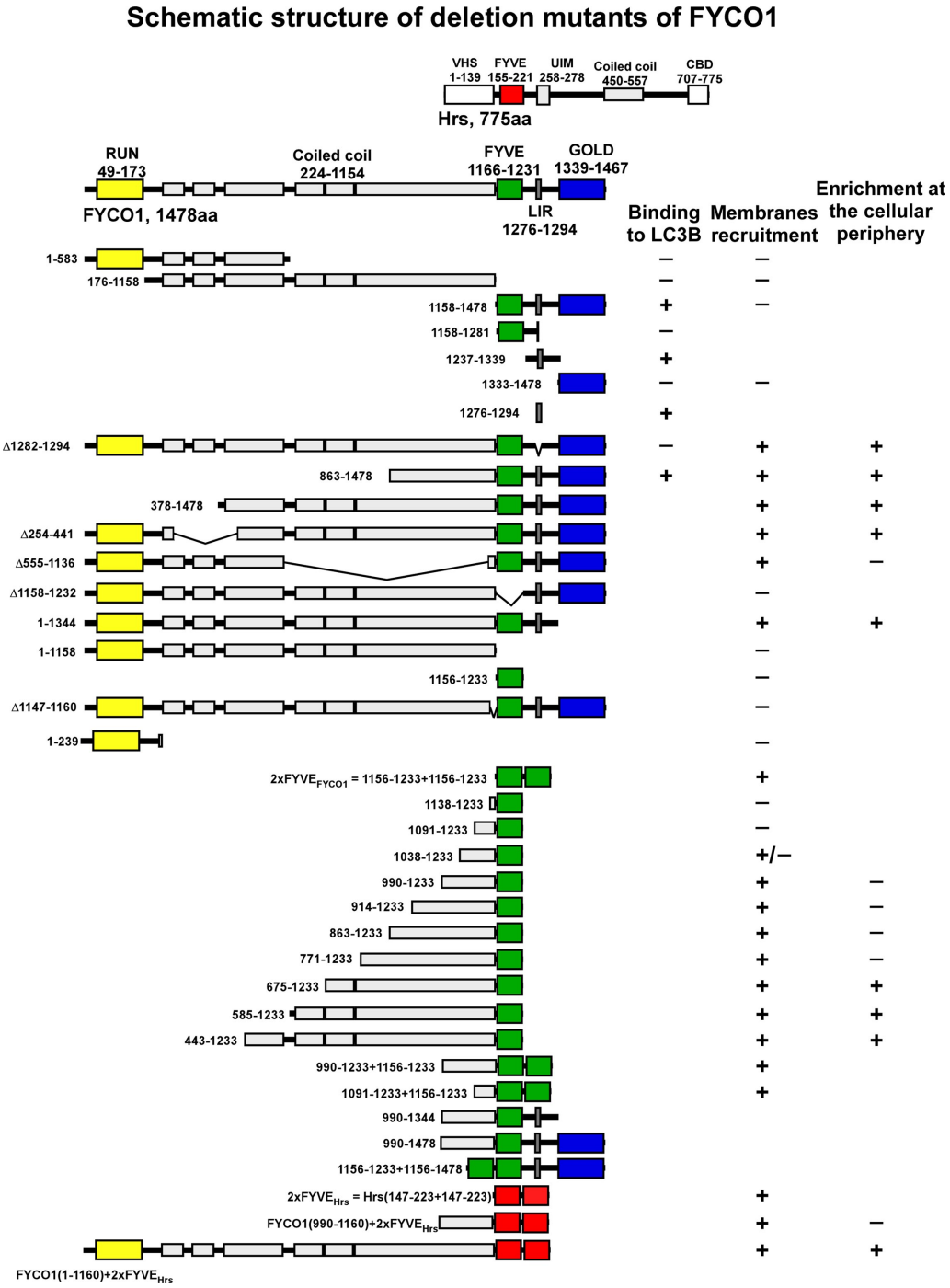

Figure S1. **Schematic structure of the deletion mutants of FYCO1.**

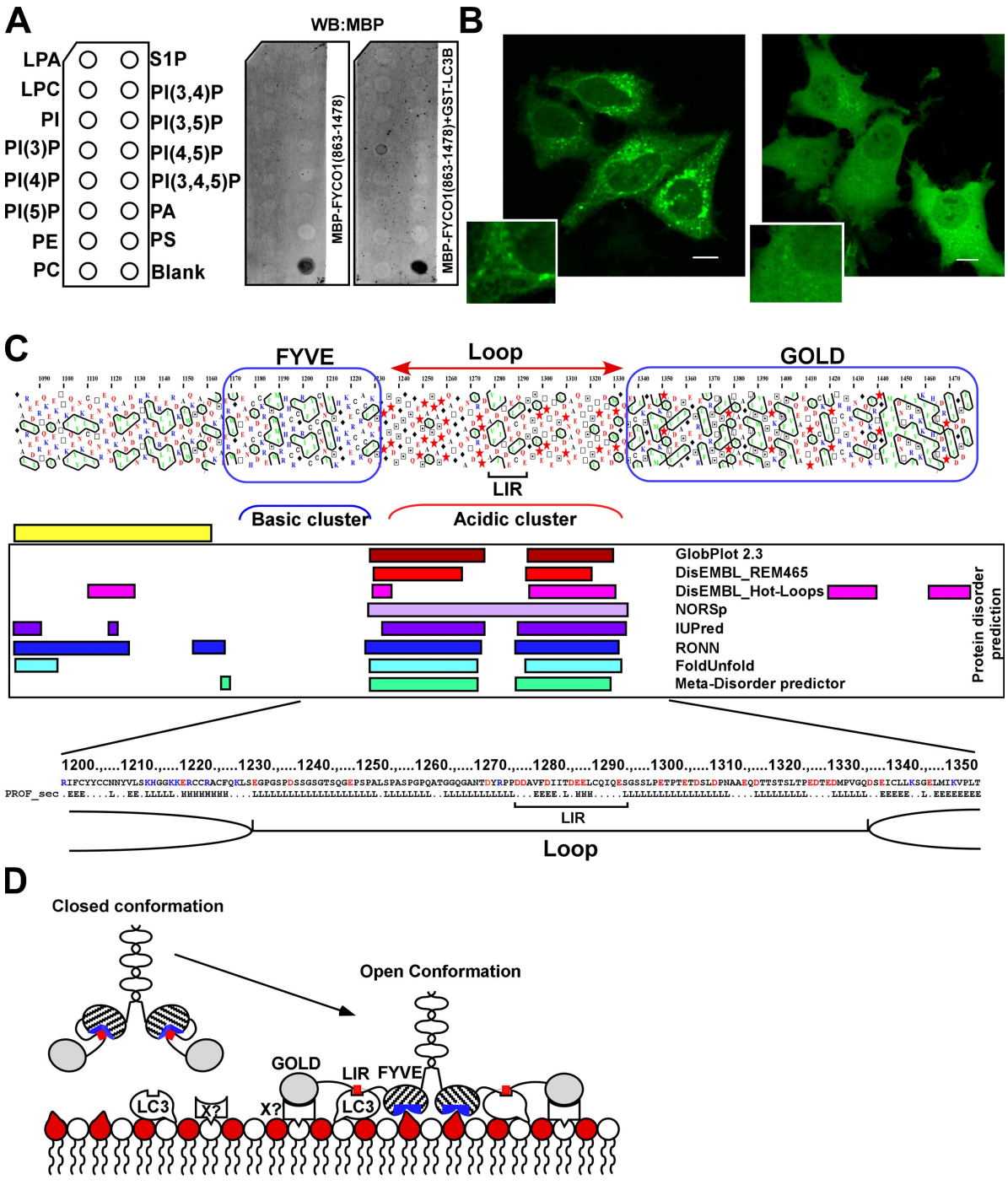

Figure S2. **The linker region between the FYVE and GOLD domains of FYCO1 has an inhibitory effect on the membrane recruitment of FYCO1.** (A) MPB-FYCO1$_{863–1,478}$ preincubated with GST-LC3B but not MBP-FYCO1$_{863–1,478}$ alone can bind to PI3P in a protein–lipid overlay assay. PIP Strips were incubated with solutions of 1 µg/ml of recombinant MBP-FYCO1$_{863–1,478}$ alone or 1 µg/ml FYCO1$_{863–1,478}$ together with 2 µg/ml GST-LC3B for 1 h, and bound proteins were detected by immunostaining with anti-MBP antibody. LPA, lysophosphatic acid; LPC, lysophosphocholine; PI, phosphatidylinositol; PE, phosphatidylethanolamine; PC, phosphatidylcholine; S1P, sphingosine-1-phosphate; PA, phosphatidic acid; PS, phosphatidylserine; WB, Western blot. (B) The region of FYCO1 between aa 1,233 and 1,344 has an inhibitory effect on the intracellular membranes recruitment. HeLa cells were transiently transfected with GFP-FYCO1$_{990–1,233}$L1151A/W1152A (left) or GFP-FYCO1$_{990–1,344}$L1151A/W1152A (right) and imaged by confocal microscopy 24 h after transfection. Insets show an enlarged field of interest. (C) The region of FYCO1 between aa 1,233 and 1,335 has properties of an acidic unstructured loop. The sequence of FYCO1 was subjected to hydrophobic cluster analysis (Mobyle@RPBS web server), CC prediction (COILS web server), secondary structure prediction (PROF, PredictProtein web server), and protein disorder prediction (GlobPlot2.3, DisEMBL, NORSp, IUPred, RONN, FoldUnfold, and Meta-Disorder prediction web servers). Red was used to highlight acidic amino acids in the sequence, whereas blue was used to highlight basic amino acids. (D) Proposed model for the regulation of membrane recruitment of FYCO1. In the absence of LC3 binding, the acidic loop between the FYVE and GOLD domains of FYCO1 folds onto the basic lipid-interacting surface of the FYVE domain and maintains FYCO1 in a lipid-unbound state. Upon the binding of LC3 to LIR in FYCO1, the acidic loop moves away from the FYVE domain, exposing the lipid interaction surface for binding to membranes. Bars, 10 µm.

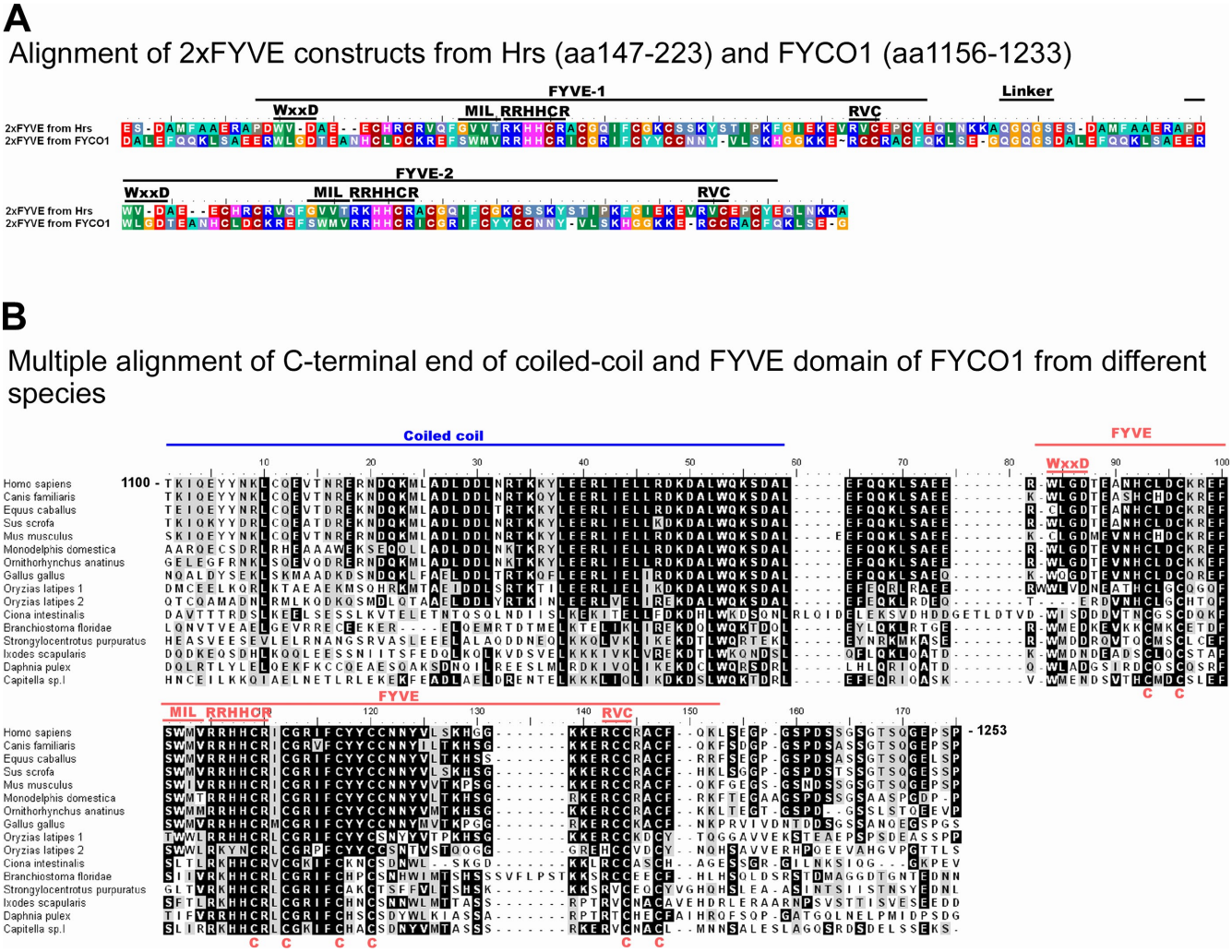

Figure S3. **FYVE domain alignments.** (A) Pairwise alignment of the protein sequences 2xFYVE$_{Hrs}$ and 2xFYVE$_{FYCO1}$. (B) Multiple sequence alignment of the C-terminal end of the CC region and FYVE domain of FYCO1 from different species. The borders of the CC, FYVE domains, and linker region as well as conserved FYVE domain–specific motifs are specified on top of the alignments. In the multialignment sequences, identity is indicated by black highlighting, and residues highlighted in gray indicate substitutions to chemically similar amino acids in more than 50% of the compared sequences.

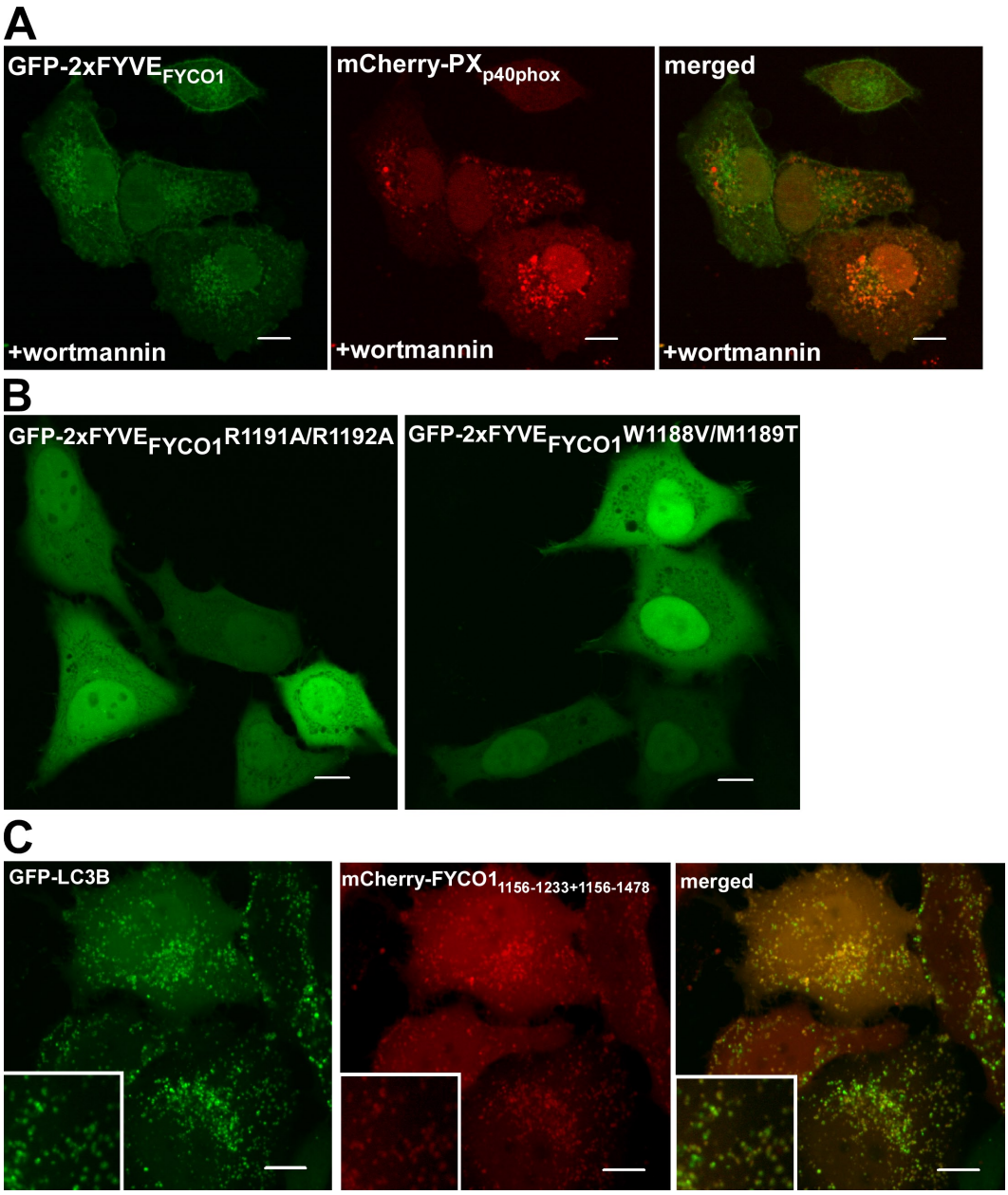

Figure S4. **Subcellular distribution of some FYVE domain–containing constructs of FYCO1.** (A) 2xFYVE from FYCO1 is partially released from the nuclear envelope and ER membranes after the inhibition of PI3P synthesis. HeLa cells were transiently transfected with the indicated constructs and were treated with 200 nM wortmannin for 1 h 24 h after transfection. (B) Exchange of the FYCO1-specific MIL FSWMV with the EEA1-specific FSVTV or mutation of the PI3P-binding motif RRHHCR to AAHHCR each impairs the membrane recruitment of 2xFYVE$_{FYCO1}$. HeLa cells were transiently transfected with the indicated constructs and imaged by confocal microscopy 24 h after transfection. (C) FYCO1$_{1,156–1,233+1,156–1,478}$ colocalizes with LC3B in the cytosolic punctuated structures. HeLa cells were transiently transfected with the indicated constructs and imaged by confocal microscopy 48 h after transfection. Insets show an enlarged field of interest. Bars, 10 µm.

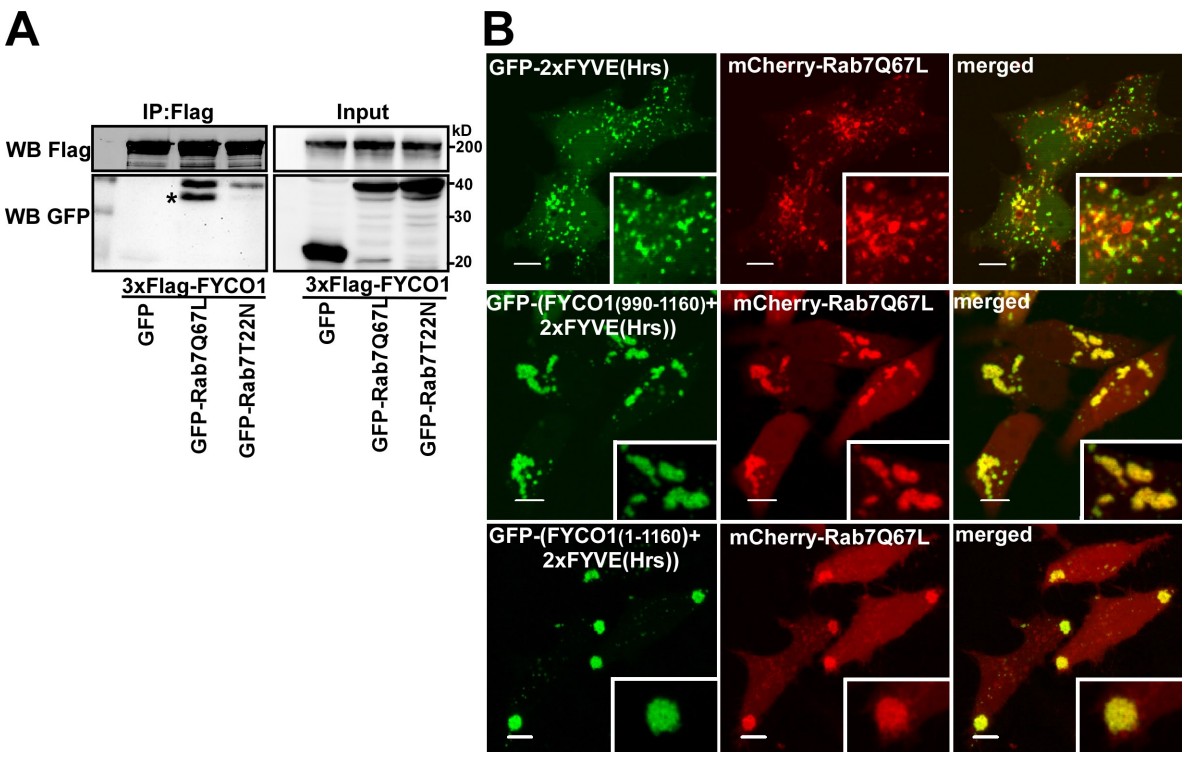

Figure S5. **FYCO1 interacts preferentially with the GTP-locked form of Rab7.** (A) Coimmunoprecipitations of transiently transfected GFP, GFP-Rab7Q67L, or GFP-Rab7T22N with 3xFlag-FYCO1 stably expressed in HEK293 FlpIn cells. The asterisk denotes a proteolytic cleavage product of GFP-Rab7Q67L. IP, immunoprecipitation; WB, Western blot. (B) The Rab7 recruitment properties of the CC region of FYCO1 can be transferred to other proteins. The fusion constructs containing the CC (aa 990–1,160) or N-terminal fragment (aa 1–1,160) of FYCO1 and 2xFYVE$_{Hrs}$ were transiently transfected into HeLa cells together with a GTP-locked mutant of Rab7, and cells were imaged 24 h after transfection. Insets show an enlarged field of interest. Bars, 10 µm.

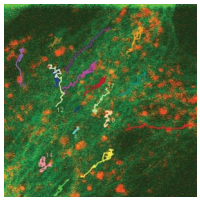

Video 1. **Movement of mCherry-FYCO1–positive vesicles along GFP-tubulin–decorated MTs.** HeLa cells were transfected with GFP-tubulin (green) and mCherry-FYCO1 and imaged by time-lapse confocal microscopy 48 h after transfection using a laser-scanning confocal microscope (LSM510; Carl Zeiss, Inc). Frames were taken every 5.93 s for 468.7 s and are presented at a frame rate of 20 frames/s. The colored numbers and their associated squiggly lines represent the 8-min-long tracks of movement of the FYCO1-decorated structures acquired with the ImageJ MTrackJ plug-in.

Table S1. **Plasmids used in this study**

Plasmids	Description	Source or reference
Gateway cloning vectors		
pENTR1A	Entry vector	Invitrogen
pENTR2B	Entry vector	Invitrogen
pENTR3C	Entry vector	Invitrogen
pDest15	Bacterial GST fusion expression vector; T7 promoter	Invitrogen
pDEST-TH1	Bacterial MBP fusion expression vector; tac promoter	Hammarström et al., 2002
pDestEGFP-C1	Mammalian EGFP fusion expression vector; CMV promoter	Lamark et al., 2003
pDestmCherry-C1	Mammalian mCherry fusion expression vector; backbone as pDestEGFP-C1	Pankiv et al., 2007
pDest53	Mammalian GFP fusion expression vector; CMV and T7 promoters	Invitrogen
pDest-myc	Mammalian myc tag fusion expression vector; CMV and T7 promoters	Lamark et al., 2003
pDestECFP-C1	Mammalian ECFP fusion expression vector; CMV promoter	Simpson et al., 2000
Other vectors		
pEGFP-C1	Mammalian EGFP fusion expression vector; CMV promoter	Takara Bio Inc.
pGEX-2T	Bacterial GST fusion expression vector; tac promoter	GE Healthcare
pAcGFP–α-tubulin	Mammalian expression vector for human α-tubulin N-terminally tagged with GFP	Takara Bio Inc.
pEGFP-ORP1L	Human ORP1L in pEGFP-C1 vector	Johansson et al., 2005
pEGFP-C1-LC3B	Human LC3B in pEGFP-C1 vector	Simonsen, et al., 2004
pmCherry-LC3B	Human LC3B N-terminally tagged with mCherry	Pankiv et al., 2007
pEGFP-2xFYVE$_{Hrs}$	Tandem fusion of FYVE domains of mHrs N-terminally tagged with EGFP	Gillooly et al., 2000
cDNA constructs made by Gateway LR reaction (previously published)		
pDest-myc-p62	Wild-type human p62 cDNA with an N-terminal myc tag in pDest-myc	Lamark et al., 2003
pDest15-LC3B	Human LC3B fused to GST in pDest15	Pankiv et al., 2007
pDest15-LC3B$_{1–28}$	N-terminal aa 1–28 of LC3B fused to GST in pDest15	Pankiv et al., 2007
pDest15-LC3B$_{30–125}$	aa 30–125 of LC3B fused to GST in pDest15	Pankiv et al., 2007
pDest15-p62K7A/D69A	Double mutant of p62 fused to GST in pDest15	Pankiv et al., 2007

CMV, cytomegalovirus.

Table S2. **Description of some of the cDNA constructs made by traditional subcloning or site-directed mutagenesis in this study**

Plasmids	Description
pEGFP-N1-FYCO1	Mammalian expression vector for human FYCO1 C-terminally tagged with EGFP
pTagFP635-N1-FYCO1	Mammalian expression vector for human FYCO1 C-terminally tagged with mKate
pcDNA5FRT/TO-EGFP-FYCO1	FlpIn mammalian expression vector for GFP-FYCO1 fusion; CMV/TetO2 promoter
pcDNA5FRT/TO-3xFlag-FYCO1	FlpIn mammalian expression vector for 3xFlag-FYCO1 fusion; CMV/TetO2 promoter
pEGFP-N1-Sar1A	Mammalian expression vector for human Sar1A C-terminally tagged with EGFP
pENTR-PX$_{p40phox}$	PX domain from human p40phox (aa 2–149) in pENTR vector
pENTR-FYCO1	Human FYCO1 (from clone DKFZp451I106) in pENTR vector
pENTR-FYCO1$_{1,276–1,294}$	LIR from FYCO1 (aa 1,276–1,294) in pENTR vector
pENTR-FYCO1$_{Δ1,282–1,294}$	FYCO1$_{ΔLIR}$ in pENTR vector
pENTR-FYCO1$_{1,156–1,233}$	FYVE domain from FYCO1 in pENTR vector
pENTR-FYCO1$_{1,156–1,233+1,156–1,233}$	2xFYVE$_{FYCO1}$ tandem fusion of two FYVE domains from FYCO1 in pENTR vector
pENTR-FYCO1$_{990–1,233+1,156–1,233}$	As 2xFYVE$_{FYCO1}$, but has aa 990–1,155 from FYCO1 in front of the first FYVE domain
pENTR-FYCO1$_{1,091–1233+1,156–1,233}$	As 2xFYVE$_{FYCO1}$, but has aa 1,091–1,155 from FYCO1 in front of the first FYVE domain
pENTR-FYCO1$_{1,156–1,233+1,156–1,478}$	As 2xFYVE$_{FYCO1}$, but has aa 1,234–1,478 from FYCO1 after the second FYVE domain
pENTR-FYCO1$_{1–1,160}$ + 2xFYVE$_{Hrs}$	FYCO1 fragment (aa 1–1,160) fused to the 2xFYVE$_{Hrs}$ from pEGFP-2xFYVE$_{Hrs}$
pENTR-FYCO1$_{990–1,160}$ + 2xFYVE$_{Hrs}$	FYCO1 fragment (aa 990–1,160) fused to the 2xFYVE$_{Hrs}$ from pEGFP-2xFYVE$_{Hrs}$

CMV, cytomegalovirus.

Other cDNA constructs made by traditional subcloning or site-directed mutagenesis in this study are as follows: pENTR-FYCO1$_{1–239}$, pENTR-FYCO1$_{1–583}$, pENTR-FYCO1$_{1–1,158}$, pENTR-FYCO1$_{1–1,344}$, pENTR-FYCO1$_{176–1,158}$, pENTR-FYCO1$_{378–1,478}$, pENTR-FYCO1$_{443–1,233}$, pENTR-FYCO1$_{585–1,233}$, pENTR-FYCO1$_{675–1,233}$, pENTR-FYCO1$_{771–1,233}$, pENTR-FYCO1$_{863–1,233}$, pENTR-FYCO1$_{863–1,478}$, pENTR-FYCO1$_{914–1,233}$, pENTR-FYCO1$_{990–1,233}$, pENTR-FYCO1$_{1,038–1,233}$, pENTR-FYCO1$_{1,091–1,233}$, pENTR-FYCO1$_{1,138–1,233}$, pENTR-FYCO1$_{1,158–1,281}$, pENTR-FYCO1$_{1,237–1,339}$, pENTR-FYCO1$_{1,333–1,478}$, pENTR-FYCO1$_{\Delta254–441}$, pENTR-FYCO1$_{\Delta555–1,136}$, pENTR-FYCO1$_{\Delta1,147–1,160}$, pENTR-FYCO1$_{\Delta1,158–1,232}$, pENTR-FYCO1R1191A/R1192A, pENTR-FYCO1$_{990–1,233}$L1151A/W1152A, pENTR-FYCO1$_{990–1,344}$L1151A/W1152A, pENTR-FYCO1$_{990–1,478}$L1151A/W1152A, pENTR-2xFYVE$_{FYCO1}$R1191A/R1192A, pENTR-2xFYVE$_{FYCO1}$W1188V/M1189T, pENTR-Rab5, pENTR-Rab5Q79L, pENTR-Rab7, pENTR-Rab7Q67L, pENTR-Rab7T22N, pENTR-Rab11, pENTR-Rab11Q70L, pENTR-Rab24, pENTR-Rab24S67L, pENTR-Rab33B, pENTR-EYFP-p62, pENTR-RILP, and pENTR-Atg5.

cDNA constructs made by Gateway LR reactions in this study are as follows: pDest53-FYCO1, pDest53-FYCO1$_{1–583}$, pDest53-FYCO1$_{176–1,158}$, pDest53-FYCO1$_{675–1,233}$, pDest53-FYCO1$_{771–1,233}$, pDest53-FYCO1$_{863–1,233}$, pDest53-FYCO1$_{914–1,233}$, pDest53-FYCO1$_{990–1,233}$, pDest53-FYCO1$_{1,038–1,233}$, pDest53-FYCO1$_{1,091–1,233}$, pDest53-FYCO1$_{1,138–1,233}$, pDest53-FYCO1$_{1,156–1,233}$, pDest53-FYCO1$_{1,158–1,281}$, pDest53-FYCO1$_{1,158–1,478}$, pDest53-FYCO1$_{1,237–1,339}$, pDest53-FYCO1$_{1,276–1,294}$, pDest53-FYCO1$_{1,333–1,478}$, pDest53-FYCO1$_{\Delta1,282–1,294}$, pDestEGFP-FYCO1, pDestEGFP-FYCO1$_{1–1,158}$, pDestEGFP-FYCO1$_{1–1,343}$, pDestEGFP-FYCO1$_{378–1,478}$, pDestEGFP-FYCO1$_{443–1,233}$, pDestEGFP-FYCO1$_{585–1,233}$, pDestEGFP-FYCO1$_{675–1,233}$, pDestEGFP-FYCO1$_{771–1,233}$, pDestEGFP-FYCO1$_{863–1,233}$, pDestEGFP-FYCO1$_{914–1,233}$, pDestEGFP-FYCO1$_{990–1,233}$, pDestEGFP-FYCO1$_{1,038–1,233}$, pDestEGFP-FYCO1$_{1,156–1,233}$, pDestEGFP-FYCO1$_{1,158–1,478}$, pDestEGFP-FYCO1$_{\Delta254–441}$, pDestEGFP-FYCO1$_{\Delta555–1,136}$, pDestEGFP-FYCO1$_{\Delta1,147–1,160}$, pDestEGFP-FYCO1$_{\Delta1,158–1,232}$, pDestEGFP-FYCO1$_{\Delta1,282–1,294}$, pDestEGFP-FYCO1$_{1,091–1,233}$, pDestEGFP-FYCO1$_{990–1,233}$L1151A/W1152A, pDestEGFP-FYCO1$_{990–1,344}$L1151A/W1152A, pDestEGFP-FYCO1$_{990–1,478}$L1151A/W1152A, pDestEGFP-FYCO1$_{990–1,233+1,156–1,233}$, pDestEGFP-FYCO1$_{1,091–1,233+1,156–1,233}$, pDestEGFP-FYCO1$_{1,156–1,233+1,156–1,233}$, pDestmCherry-FYCO1, pDestmCherry-FYCO1$_{\Delta555–1,136}$, pDestmCherry-FYCO1$_{1,156–1,233+1,156–1,233}$, pDestmCherry-FYCO1$_{1,156–1,233+1,156–1,478}$, pDest-myc-FYCO1, pDest-myc-FYCO1$_{1–239}$, pDest-myc-FYCO1$_{1–583}$, pDest-myc-FYCO1$_{175–1,158}$, pDest-myc-FYCO1$_{585–1,233}$, pDest-myc-FYCO1$_{1,158–1,478}$, pDEST-TH1-FYCO1$_{863–1,233}$, pDEST-TH1-FYCO1$_{863–1,478}$, pDEST-TH1-FYCO1$_{1,156–1,233}$, pDEST-TH1-FYCO1$_{1,156–1,233+1,156–1,233}$, pDestEGFP-Rab5, pDestEGFP-Rab5Q79L, pDestEGFP-Rab7, pDestEGFP-Rab7Q67L, pDestEGFP-Rab7T22N, pDestmCherry-Rab7Q67L, pDestEGFP-Rab11, pDestEGFP-Rab11Q70L, pDestEGFP-Rab24, pDestEGFP-Rab24S67L, pDestEGFP-Rab33B, pDestEGFP-RILP, pDestmCherry-EYFP-p62, pDestmCherry-PX$_{p40phox}$, pDestmCherry-HttQ68, and pDestmCherry-Atg5.

References

Gillooly, D.J., I.C. Morrow, M. Lindsay, R. Gould, N.J. Bryant, J.M. Gaullier, R.G. Parton, and H. Stenmark. 2000. Localization of phosphatidylinositol 3-phosphate in yeast and mammalian cells. *EMBO J.* 19:4577–4588. doi:10.1093/emboj/19.17.4577

Hammarström, M., N. Hellgren, S. van Den Berg, H. Berglund, and T. Härd. 2002. Rapid screening for improved solubility of small human proteins produced as fusion proteins in *Escherichia coli*. *Protein Sci.* 11:313–321. doi:10.1110/ps.22102

Johansson, M., M. Lehto, K. Tanhuanpää, T.L. Cover, and V.M. Olkkonen. 2005. The oxysterol-binding protein homologue ORP1L interacts with Rab7 and alters functional properties of late endocytic compartments. *Mol. Biol. Cell.* 16:5480–5492. doi:10.1091/mbc.E05-03-0189

Lamark, T., M. Perander, H. Outzen, K. Kristiansen, A. Øvervatn, E. Michaelsen, G. Bjørkøy, and T. Johansen. 2003. Interaction codes within the family of mammalian Phox and Bem1p domain-containing proteins. *J. Biol. Chem.* 278:34568–34581. doi:10.1074/jbc.M303221200

Pankiv, S., T.H. Clausen, T. Lamark, A. Brech, J.A. Bruun, H. Outzen, A. Øvervatn, G. Bjørkøy, and T. Johansen. 2007. p62/SQSTM1 binds directly to Atg8/LC3 to facilitate degradation of ubiquitinated protein aggregates by autophagy. *J. Biol. Chem.* 282:24131–24145. doi:10.1074/jbc.M702824200

Simonsen, A., H.C. Birkeland, D.J. Gillooly, N. Mizushima, A. Kuma, T. Yoshimori, T. Slagsvold, A. Brech, and H. Stenmark. 2004. Alfy, a novel FYVE-domain-containing protein associated with protein granules and autophagic membranes. *J. Cell Sci.* 117:4239–4251. doi:10.1242/jcs.01287

Simpson, J.C., R. Wellenreuther, A. Poustka, R. Pepperkok, and S. Wiemann. 2000. Systematic subcellular localization of novel proteins identified by large-scale cDNA sequencing. *EMBO Rep.* 1:287–292. doi:10.1093/embo-reports/kvd058